

## Supramolecular Chemistry

**Reaction-Temperature-Dependent Supramolecular Isomerism of Coordination Networks Based on the Organometallic Building Block  $[\text{Cu}^{\text{I}}_2(\mu_2\text{-BQ})(\mu_2\text{-OAc})_2]$ \*\***

Shigeyuki Masaoka, Daisuke Tanaka,  
Yasunori Nakanishi, and Susumu Kitagawa\*

Much effort has been devoted to the design and controlled crystallization of coordination networks based on transition-metal atoms and multifunctional bridging ligands owing to their potential applications such as magnetism, electric conductivity, molecular adsorption, and heterogeneous catalysis. Supramolecular isomerism, the existence of more than one superstructure for given set of components, is of particular importance because the superstructure plays an essential role in determining the properties of crystalline materials.<sup>[1]</sup> All phenomena regarding supramolecular isomerism in coordination networks reported so far show crystal structures that contain solvent (guest) molecules to satisfy crystal packing, which result from different stoichiometry of the included solvent.<sup>[2]</sup> Therefore, these are categorized as a group of solvent-induced (guest-induced) pseudo-polymorphism. In spite of many investigations, no examples have been reported of supramolecular isomerism with a fixed stoichiometry for all components, which would lie at the very heart of the concept of supramolecular isomerism. Herein we

[\*] S. Masaoka, D. Tanaka, Y. Nakanishi, Prof. S. Kitagawa  
Department of Synthetic Chemistry and Biological Chemistry  
Graduate School of Engineering  
Kyoto University  
Katsura, Nishikyo-ku, Kyoto 615-8510 (Japan)  
Fax: (+81) 75-383-2732  
E-mail: kitagawa@sbchem.kyoto-u.ac.jp

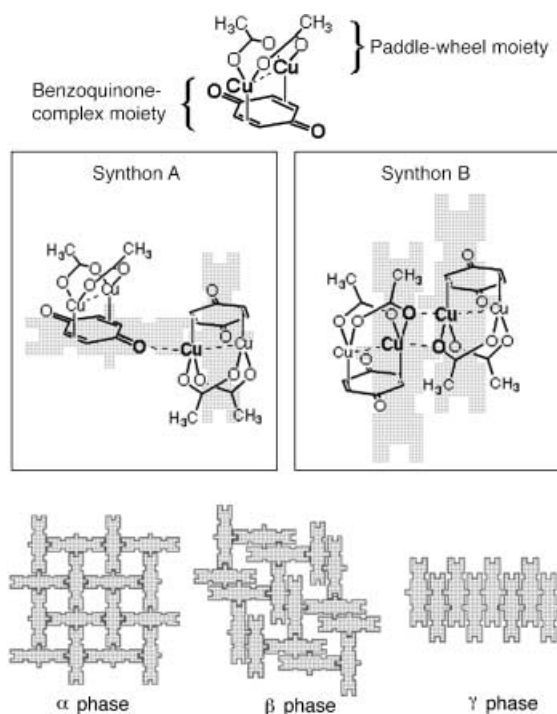
[\*\*] This work was partially supported by the Japan Society for the Promotion of Science. BQ = *p*-benzoquinone



Supporting information for this article is available on the WWW under <http://www.angewandte.org> or from the author.

report three supramolecular isomers without any solvent molecules. Interestingly, these three isomers were crystallized in the same solvent. This result is expected to afford important information for modern crystal engineering.

$[\text{Cu}^{\text{I}}_2(\mu_2\text{-BQ})(\mu_2\text{-OAc})_2]$  (BQ = *p*-benzoquinone) was obtained by the redox reaction between dimetallic copper(II) acetate,  $[\text{Cu}^{\text{II}}_2(\text{OAc})_4(\text{H}_2\text{O})_2]$ , as oxidant, and hydroquinone (HQ) as reductant.<sup>[3]</sup> The use of this organometallic building block is a key to the formation of supramolecular isomers because this complex has two types of supramolecular synthons on coordination (Scheme 1).<sup>[4]</sup> Because the building



**Scheme 1.** Top: two types of supramolecular synthon on coordination between two dicopper building blocks. Bottom: Schematic representation of three supramolecular isomers.

block has two oxygen atoms from the benzoquinone moiety, the lone pairs of the oxygen atoms can coordinate metal ions (synthon A in Scheme 1).<sup>[5]</sup> On the other hand, a half of the complex looks like a paddle-wheel structure, and functions as a molecular building block with a mutual metal–oxygen coordinating group (synthon B in Scheme 1). Therefore, the infinite assembly of this organometallic building block could afford a variety of supramolecular isomers owing to competition between the two different intermolecular interactions.

The redox reaction of dimetallic copper(II) acetate,  $[\text{Cu}^{\text{II}}_2(\text{OAc})_4(\text{H}_2\text{O})_2]$  (2 g) with hydroquinone (HQ; 2.2 g) in ethanol (100 mL) affords a red solution of the molecular building block  $[\text{Cu}^{\text{I}}_2(\mu_2\text{-BQ})(\mu_2\text{-OAc})_2]$ . When the solution was left at room temperature, two supramolecular isomers,  $[\text{Cu}^{\text{I}}_2(\mu_4\text{-BQ})(\mu_2\text{-OAc})_2]_n$  ( $\alpha$  phase) and  $[\text{Cu}^{\text{I}}_2(\mu_3\text{-BQ})(\mu_2\text{-OAc})_2]_n$  ( $\beta$  phase), were obtained as thin and thick plates, respectively (Figure 1 a and Figure 2 a). On the other hand, when the reaction temperature was fixed at 60 °C, red

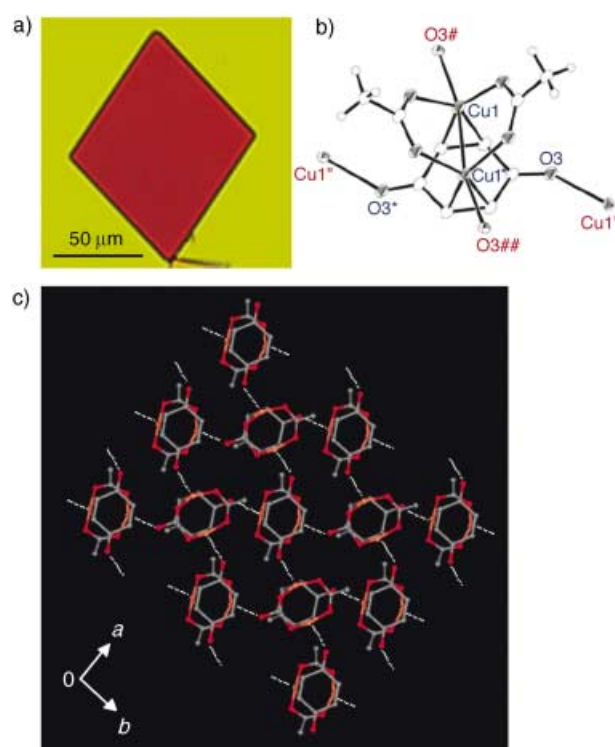


**Figure 1.** a) Photograph of a single crystal of the  $\alpha$  phase. b) Structure of the building block with the nearest-neighbor coordinated atoms in the  $\alpha$  phase. The distance of the Cu1–O3# bond is 2.270(3) Å. c) Infinite structure of the two-dimensional sheet of the  $\alpha$  phase.

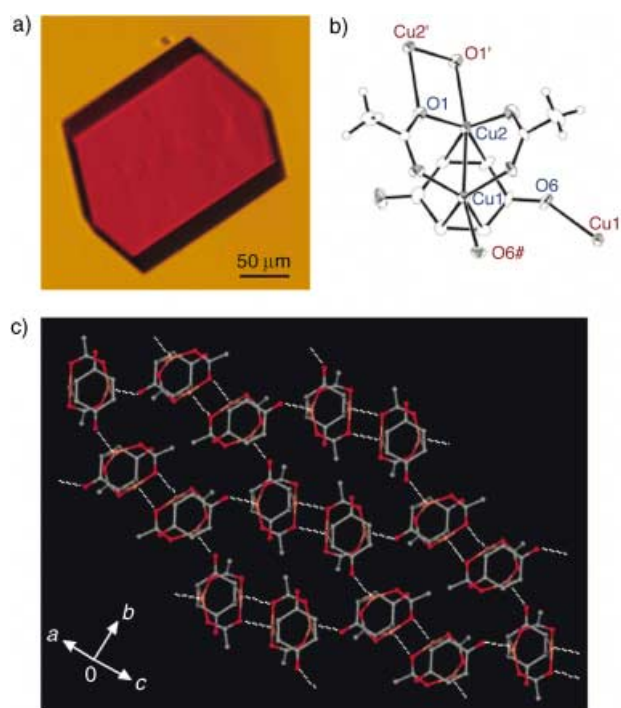


**Figure 2.** a) Photograph of a single crystal of the  $\beta$  phase. b) Structure of the building block with the nearest-neighbor coordinated atoms in the  $\beta$  phase. The distances of the Cu1–O6# bond and the Cu2–O1' bond are 2.254(3) and 2.278(2) Å, respectively. c) Infinite structure of the two-dimensional sheet of the  $\beta$  phase.

columns of  $[\text{Cu}^{\text{I}}_2(\mu_2\text{-BQ})(\mu_3\text{-OAc})_2]_n$  ( $\gamma$  phase) were mainly obtained with red plates of  $\beta$  phase as a minor product (Figure 3a). All compounds were characterized by X-ray crystallography.<sup>[6]</sup>

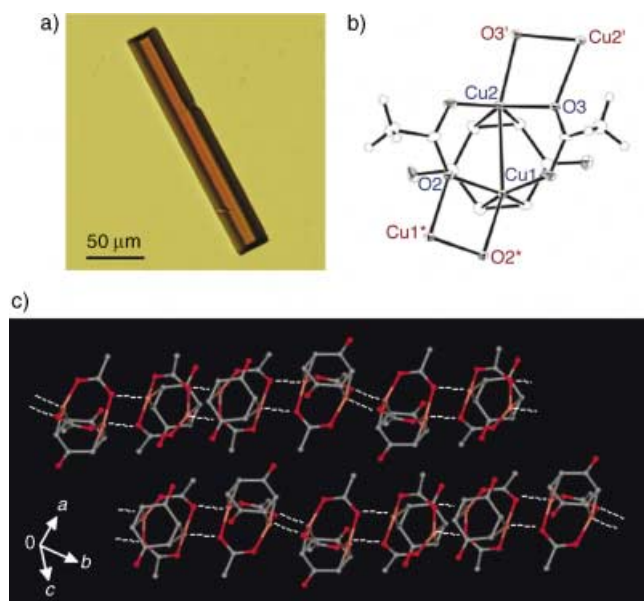


**Figure 3.** a) Photograph of a single crystal of the  $\gamma$  phase. b) Structure of the building block with the nearest-neighbor coordinated atoms in the  $\gamma$  phase. The distances of the  $\text{Cu1}-\text{O2}^*$  bond and the  $\text{Cu2}-\text{O3}'$  bond are 2.233(4) and 2.227(4) Å, respectively. c) Infinite structure of the one-dimensional chain of the  $\gamma$  phase.

The X-ray diffraction of a red thin plate of the  $\alpha$  phase shows orthorhombic space group ( $P2_12_12$ , no. 18).<sup>[7]</sup> The crystal structure of the  $\alpha$  phase is shown in Figure 1. The building block  $[\text{Cu}^{\text{I}}_2(\text{BQ})(\text{OAc})_2]$  has approximately  $C_{2v}$  symmetry in the crystals of the  $\alpha$  phase (see Supporting Information). Figure 1b focuses on the building block with the nearest-neighbor coordinated atoms. The oxygen atoms of the BQ coordinate the axial positions of the dicopper cores of the neighboring building blocks ( $\text{Cu1}-\text{O3}^\#$ : 2.270(3) Å). Consequently, the BQ ligands have  $\mu_4$  coordination geometry, resulting in the formation of a 2D sheet (Figure 1c). As shown in Figure 1c, one building block adjoins four other building blocks in the  $\alpha$  phase.

Red plates of the  $\beta$  phase have monoclinic space group ( $P2_1/n$ , no. 14).<sup>[8]</sup> The crystal structure of the  $\beta$  phase is shown in Figure 2. The dicopper building block remains approximately  $C_{2v}$  symmetry in the crystals of the  $\beta$  phase (see Supporting Information). One of the two axial positions of the dicopper core is occupied by the oxygen atom from the BQ ligand of the neighboring building block, and the other is occupied by the oxygen atom from the  $\text{AcO}^-$  ligand of the neighboring building block (Figure 2b). The  $\text{Cu1}-\text{O6}^\#$  (BQ) bond length is 2.254(3) Å and that of  $\text{Cu2}-\text{O1}'$  ( $\text{AcO}^-$ ) bond is 2.278(2) Å. As a result, the benzoquinone ligand functions as a  $\mu_3$  bridging ligand, and two  $\text{AcO}^-$  ligands act as  $\mu_2$  and  $\mu_3$  bridging ligands, thus affording the formula  $[\text{Cu}^{\text{I}}_2(\mu_3\text{-BQ})(\mu_2\text{-OAc})(\mu_3\text{-OAc})]_n$ . Figure 2c illustrates the infinite structure of

the two-dimensional sheet of the  $\beta$  phase. In  $\beta$  phase, one building block adjoins three other building blocks to form a two-dimensional sheet.

The X-ray diffraction of a red column of  $\gamma$  phase shows orthorhombic space group ( $Pccn$ , no. 56).<sup>[9]</sup> The crystal structure of  $\gamma$  phase is shown in Figure 3. The illustration of the dicopper building block along Cu–Cu axis (see Supporting Information) clearly shows the distortion from the ideal  $C_{2v}$  symmetrical structure in the crystals of the  $\gamma$  phase. The Cu–Cu distance of the  $\gamma$  phase (2.7530(9) Å) is longer than those of  $\alpha$  and  $\beta$  phases (2.7207(9) and 2.7232(7) Å, respectively). Figure 3b reveals a dicopper unit with the nearest-neighbor coordinated atoms in the crystals of the  $\gamma$  phase. The axial positions of the dicopper core are occupied by the oxygen atoms from the  $\text{AcO}^-$  ligands of the neighboring building blocks ( $\text{Cu1}-\text{O2}''$ : 2.233(4) Å,  $\text{Cu2}-\text{O3}'$ : 2.227(4) Å). The two  $\text{AcO}^-$  ligands in  $\gamma$  phase act as  $\mu_3$  bridging ligands, forming one-dimensional chain. In the case of  $\gamma$  phase, one building block adjoins two other building blocks.

Pure  $\alpha$ ,  $\beta$ , and  $\gamma$  phases were isolated as microcrystals by varying the reaction temperature and concentration. Pure  $\alpha$  phase was obtained in a 82 % yield when the reaction temperature was fixed at 30 °C, with 250 mm of  $[\text{Cu}^{\text{I}}_2(\text{OAc})_4(\text{H}_2\text{O})_2]$  and 1 M of HQ in ethanol.<sup>[10]</sup> When the reaction temperature was fixed at 40 °C, with 50 mm of  $[\text{Cu}^{\text{I}}_2(\text{OAc})_4(\text{H}_2\text{O})_2]$  and 200 mm of HQ in ethanol, pure  $\beta$  phase was isolated in a 34 % yield.<sup>[11]</sup> When the mixture of 50 mm of  $[\text{Cu}^{\text{I}}_2(\text{OAc})_4(\text{H}_2\text{O})_2]$  and 200 mm of HQ in EtOH was heated to reflux, pure  $\gamma$  phase was obtained in an 87 % yield.<sup>[12]</sup>

The distortion of the building block in  $\gamma$  phase compared with  $\alpha$  and  $\beta$  phases clearly influences spectroscopic properties of these supramolecular isomers. The IR spectra of all isomers show a bathochromic shift of the stretching frequency  $\nu(\text{C}=\text{O})$  of the BQ as compared to the free BQ ( $\tilde{\nu} = 1662 \text{ cm}^{-1}$ ), the magnitude of which depends on the type of isomers. In the  $\gamma$  phase,  $\nu(\text{C}=\text{O})$  is only slightly shifted ( $\tilde{\nu} = 1652 \text{ cm}^{-1}$ ,  $\Delta\tilde{\nu} = 10 \text{ cm}^{-1}$ ), whereas in the  $\alpha$  and  $\beta$  phases the shifts are approximately  $30 \text{ cm}^{-1}$  ( $\alpha$  phase:  $\tilde{\nu} = 1632 \text{ cm}^{-1}$ ,  $\Delta\tilde{\nu} = 30 \text{ cm}^{-1}$ ,  $\beta$ -phase:  $\tilde{\nu} = 1629, 1638 \text{ cm}^{-1}$ ,  $\Delta\tilde{\nu} = 33, 24 \text{ cm}^{-1}$ ). The  $^{13}\text{C}$  CPMAS NMR spectra also show differences of chemical shifts of three supramolecular isomers (Supporting Information). The chemical shifts of all corresponding carbon atoms in  $\alpha$  and  $\beta$  phases are within 1 ppm difference. On the other hand, each carbon atom in the  $\gamma$  phase shows a chemical shift different by 2–3 ppm compared with the corresponding carbon atoms in  $\alpha$  and  $\beta$  phases.

Our systematic studies of varying the reaction temperature and concentration in conjunction with supramolecular isomerism provides a map of the crystallization process of the building block  $[\text{Cu}^{\text{I}}_2(\mu_2\text{-BQ})(\mu_2\text{-OAc})_2]$  (Figure 4).<sup>[13]</sup> High-temperature reaction conditions and a low concentration (50 mm) of the molecular building block results in thermodynamically controlled crystallization such that the  $\gamma$  phase is favored. As the reaction temperature is decreased to 60 °C and with a concentration of the building block of 50 mm, a mixture of  $\beta$  phase and  $\gamma$  phase is obtained, thus indicating that the  $\beta$  phase is kinetically favored compared with the  $\gamma$  phase.<sup>[14]</sup> When the temperature is further decreased to 40 °C, only the  $\beta$  phase is obtained. As the temperature is

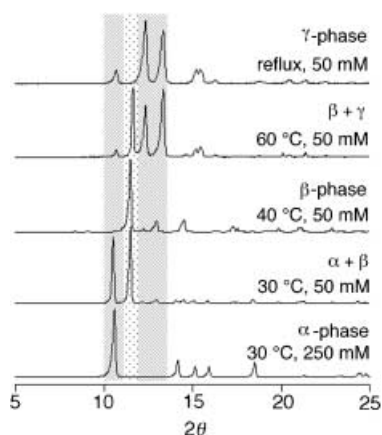


**Figure 4.** Reaction temperature- and concentration-dependent powder XRD patterns. Top, middle, and bottom lines represent powder XRD patterns of the  $\alpha$ ,  $\beta$ , and  $\gamma$  phases, respectively. The samples synthesized with a concentration of 50 mM of the building block at 60 °C and 30 °C result in the mixtures of two phases.

fixed at 30 °C and the concentration of the building block is 50 mM, the mixture of  $\alpha$  phase and  $\beta$  phase is obtained, thus indicating that the  $\alpha$  phase is the most kinetically favored product. A further decrease of temperature leads to disproportionation of the building block into copper(II) acetate and HQ, which prevents the isolation of the  $\alpha$  phase at lower temperatures. Kinetically controlled crystallization of the  $\alpha$  phase was successfully performed at 30 °C with higher concentrations of the building block (250 mM), which is associated with acceleration of the crystallization process. For this system, the synthon A is preferred to the synthon B in the kinetically controlled crystallization, while the opposite propensity is observed in thermodynamically controlled crystallization, thus resulting in the three supramolecular isomers.

Received: December 5, 2003

Revised: February 17, 2004 [Z53463]

**Keywords:** coordination polymers · polymorphism · quinines · self-assembly · supramolecular chemistry

- [1] B. Moulton, M. J. Zaworotko, *Chem. Rev.* **2001**, *101*, 1629–1658.
- [2] a) T. L. Hennigar, D. C. MacQuarrie, P. Losier, R. D. Rogers, M. J. Zaworotko, *Angew. Chem.* **1997**, *109*, 1044–1046; *Angew. Chem. Int. Ed. Engl.* **1997**, *36*, 972–973; b) D. J. Soldatov, J. A. Ripmeester, S. I. Shergina, I. E. Sokolov, A. S. Zanina, S. A. Gromilov, Y. A. Dyadin, *J. Am. Chem. Soc.* **1999**, *121*, 4179–4188; c) B. Chen, F. R. Fronczek, A. W. Maverick, *Chem. Commun.* **2003**, 2166–2167; d) K. Uemura, S. Kitagawa, M. Kondo, K. Fukui, R. Kitaura, H.-C. Chang, T. Mizutani, *Chem. Eur. J.* **2002**, *8*, 3587–3600.
- [3] S. Masaoka, G. Akiyama, S. Horike, S. Kitagawa, T. Ida, K. Endo, *J. Am. Chem. Soc.* **2003**, *125*, 1152–1153.
- [4] G. R. Desiraju, *Angew. Chem.* **1995**, *107*, 2541–2558; *Angew. Chem. Int. Ed. Engl.* **1995**, *34*, 2311–2327.
- [5] a) M. Oh, G. B. Carpenter, D. A. Sweigart, *Angew. Chem.* **2003**, *115*, 2072–2074; *Angew. Chem. Int. Ed.* **2003**, *42*, 2026–2028; b) M. Oh, G. B. Carpenter, D. A. Sweigart, *Angew. Chem.* **2002**,

- 114*, 3802–3805; *Angew. Chem. Int. Ed.* **2002**, *41*, 3650–3653; c) M. Oh, G. B. Carpenter, D. A. Sweigart, *Angew. Chem.* **2001**, *113*, 3291–3294; *Angew. Chem. Int. Ed.* **2001**, *40*, 3191–3194.
- [6] X-ray structure determination: All data of the X-ray structure determination of  $\alpha$ ,  $\beta$ , and  $\gamma$  phases were measured on Rigaku/MSD Mercury CCD diffractometer with graphite-monochromated  $\text{MoK}\alpha$  radiation. These structures were solved by direct methods and expanded by using Fourier techniques. The non-hydrogen atoms were refined anisotropically. Refinements were carried out with full-matrix least-square techniques. All calculations were performed with the TEXSAN crystallographic program. CCDC-225749 ( $\alpha$  phase), CCDC-225750 ( $\beta$  phase), and CCDC-225751 ( $\gamma$  phase) contain the supplementary crystallographic data for this paper. These data can be obtained free of charge via [www.ccdc.cam.ac.uk/conts/retrieving.html](http://www.ccdc.cam.ac.uk/conts/retrieving.html) (or from the Cambridge Crystallographic Data Centre, 12 Union Road, Cambridge CB2 1EZ, UK; fax: (+44) 1223-336-033; or deposit@ccdc.cam.ac.uk).
- [7] Crystal data for  $\alpha$ -phase,  $\text{C}_{10}\text{H}_{10}\text{Cu}_2\text{O}_6$ ;  $M_r = 353.28$ , crystal size  $0.20 \times 0.20 \times 0.01$  mm, orthorhombic, space group  $P2_12_12_1$  (no. 18),  $a = 7.438(3)$ ,  $b = 9.356(3)$ ,  $c = 8.293(3)$  Å,  $V = 577.1(3)$  Å<sup>3</sup>,  $Z = 2$ ,  $\rho_{\text{calcd}} = 2.033$  g cm<sup>-3</sup>,  $\lambda(\text{MoK}\alpha) = 0.7107$  Å,  $F(000) = 352.00$ ,  $\mu(\text{MoK}\alpha) = 37.00$  cm<sup>-1</sup>,  $T = -20^\circ\text{C}$ ,  $2\theta_{\text{max}} = 54.9^\circ$ , of the 4987 reflections that were collected, 276 were unique ( $R_{\text{int}} = 0.034$ ); equivalent reflections were merged. For 1252 reflections with  $I > 2.00\sigma(I)$ , 83 parameters;  $R(R_w) = 0.041(0.054)$ . The residual electron density (min./max.) is  $-0.87/0.93$  e<sup>-</sup> Å<sup>-3</sup>. The Flack parameter is 0.03(4).
- [8] Crystal data for  $\beta$  phase,  $\text{C}_{10}\text{H}_{10}\text{Cu}_2\text{O}_6$ ;  $M_r = 353.28$ , crystal size  $0.30 \times 0.20 \times 0.03$  mm, monoclinic, space group  $P2_1/n$  (no. 14),  $a = 10.403(4)$ ,  $b = 7.540(2)$ ,  $c = 15.543(5)$  Å,  $\beta = 103.661(7)^\circ$ ,  $V = 1184.8(7)$  Å<sup>3</sup>,  $Z = 4$ ,  $\rho_{\text{calcd}} = 1.980$  g cm<sup>-3</sup>,  $\lambda(\text{MoK}\alpha) = 0.7107$  Å,  $F(000) = 704.00$ ,  $\mu(\text{MoK}\alpha) = 36.05$  cm<sup>-1</sup>,  $T = -30^\circ\text{C}$ ,  $2\theta_{\text{max}} = 55.0^\circ$ , of the 10898 reflections which were collected, 2693 were unique ( $R_{\text{int}} = 0.043$ ); equivalent reflections were merged. For 2407 reflections with  $I > 2.00\sigma(I)$ , 163 parameters;  $R(R_w) = 0.040(0.058)$ . The residual electron density (min./max.) is  $-0.72/1.00$  e<sup>-</sup> Å<sup>-3</sup>.
- [9] Crystal data for  $\gamma$ -phase,  $\text{C}_{10}\text{H}_{10}\text{Cu}_2\text{O}_6$ ;  $M_r = 353.28$ , crystal size  $0.40 \times 0.03 \times 0.01$  mm, orthorhombic, space group  $Pccn$  (no. 56),  $a = 9.422(3)$ ,  $b = 17.301(5)$ ,  $c = 14.416(5)$  Å,  $V = 2349(1)$  Å<sup>3</sup>,  $Z = 8$ ,  $\rho_{\text{calcd}} = 1.997$  g cm<sup>-3</sup>,  $\lambda(\text{MoK}\alpha) = 0.7107$  Å,  $F(000) = 1408.00$ ,  $\mu(\text{MoK}\alpha) = 36.35$  cm<sup>-1</sup>,  $T = -30^\circ\text{C}$ ,  $2\theta_{\text{max}} = 55.0^\circ$ , of the 21865 reflections which were collected, 2678 were unique ( $R_{\text{int}} = 0.033$ ); equivalent reflections were merged. For 2033 reflections with  $I > 2.00\sigma(I)$ , 163 parameters;  $R(R_w) = 0.055(0.060)$ . The residual electron density (min./max.) is  $-0.58/1.03$  e<sup>-</sup> Å<sup>-3</sup>.
- [10]  $[\text{Cu}^{\text{II}}_2(\mu_4\text{-BQ})(\mu_2\text{-OAc})_2]_n$  ( $\alpha$ -phase): A solution of HQ (11 g) and copper(II) acetate  $[\text{Cu}^{\text{II}}_2(\text{OAc})_4(\text{H}_2\text{O})_2]$  (10 g) in ethanol (100 mL) was stirred at 30 °C for 30 min, and left at 30 °C without a stir. After 3 h red thin plates obtained were collected by filtration, washed with hexane, and dried in vacuo (82% yield). Elemental analysis calcd (%) for  $\text{C}_{10}\text{H}_{10}\text{Cu}_2\text{O}_6$ : C 34.00, H 2.85; found: C 33.93, H 2.92. An XRPD spectrum of the massive product of  $\alpha$  phase fit the profile derived from the crystal structure (see Supporting Information).
- [11]  $[\text{Cu}^{\text{II}}_2(\mu_3\text{-BQ})(\mu_2\text{-OAc})(\mu_3\text{-OAc})]_n$  ( $\beta$  phase): A colorless solution of HQ (2.2 g) in ethanol (50 mL) was added to a green solution of copper(II) acetate  $[\text{Cu}^{\text{II}}_2(\text{OAc})_4(\text{H}_2\text{O})_2]$  (2 g) in ethanol (50 mL). The mixture was stirred at 40 °C for 1 min, and left at 40 °C without stirring. After 2 h red plates obtained were collected by filtration, washed with hexane, and dried in vacuo (34% yield). Elemental analysis calcd (%) for  $\text{C}_{10}\text{H}_{10}\text{Cu}_2\text{O}_6$ : C 34.00, H 2.85; found: C 33.74, H 2.97. A powder XRD spectrum of the massive product of  $\beta$  phase fit the profile derived from the crystal structure (see Supporting Information).

- [12]  $[\text{Cu}^{\text{I}}_2(\mu_2\text{-BQ})(\mu_3\text{-OAc})_2]_n$  ( $\gamma$ -phase): A solution of HQ (2.2 g) and copper(II) acetate  $[\text{Cu}^{\text{II}}_2(\text{OAc})_4(\text{H}_2\text{O})_2]$  (2 g) in ethanol (100 mL) was heated to reflux for 1.5 h to give a red precipitate. This was isolated by filtration, washed with hexane, and dried in vacuo (87 % yield). Elemental analysis calcd (%) for  $\text{C}_{10}\text{H}_{10}\text{Cu}_2\text{O}_6$ : C 34.00, H 2.85; found: C 34.03, H 2.84. A powder XRD spectrum of the massive product of  $\gamma$  phase fit the profile derived from the crystal structure (see Supporting Information).
- [13] Experiment at 60 °C: The crystallization at 60 °C with a low concentration (50 mM) was performed as follows. A colorless solution of HQ (2.2 g) in ethanol (50 mL) and a green solution of copper(II) acetate  $[\text{Cu}^{\text{II}}_2(\text{OAc})_4(\text{H}_2\text{O})_2]$  (2 g) in ethanol (50 mL) were mixed and stirred for 1 min at 60 °C, and left without a stir for 2 h at 60 °C. The crystalline product obtained was collected by filtration, washed with hexane, and dried in vacuo. A powder XRD spectrum of the product obtained at 60 °C corresponded to the mixture of  $\beta$  and  $\gamma$  phases (Figure 4). The other experiments at 30 and 40 °C were performed in similar ways to that at 60 °C, affording the  $\alpha$ ,  $\beta$  mixture and the pure  $\beta$  phase, respectively (Figure 4).
- [14] When a solid offers several polymorphs, the metastable phase with the higher solubility tends to be kinetically favored. This empirical rule, known as the Ostwald step rule, is understood by the nucleation kinetics of the solid.<sup>[15]</sup> At a given supersaturation ratio, the activation energy of nucleation, which determines the nucleation speed, decreases in proportion as the interfacial tension decreases. Thus, because the solubility is inversely proportional to the interfacial tension, the precipitation of the more soluble phase, or the metastable phase, is therefore kinetically promoted under low temperature condition. For the system described in this paper, the difference of interaction energy between the two supramolecular synthons would cause the difference of stabilities among three crystalline phases.
- [15] A. E. Nielsen, *Kinetics of Precipitation*, Pergamon, Oxford, **1964**.